Invited review

Supercritical CO₂ fracking for enhanced shale gas recovery and CO₂ sequestration: Results, status and future challenges

Junping Zhou[1,2]ⓘ*, Nan Hu[1,2], Xuefu Xian[1,2], Lei Zhou[1,2], Jiren Tang[1,2], Yong Kang[3], Haizhu Wang[4]

[1]*State Key Laboratory of Coal Mine Disaster Dynamics and Control, Chongqing University, Chongqing 400044, P. R. China*

[2]*College of Resources and Environmental Science, Chongqing University, Chongqing 400044, P. R. China*

[3]*Key Laboratory of Hubei Province for Water Jet Theory & New Technology, Wuhan 430072, P. R. China*

[4]*State Key Laboratory of Petroleum Resources and Prospecting, China University of Petroleum, Beijing 102249, P. R. China*

Abstract:

Supercritical carbon dioxide (ScCO₂)-based fracturing technology associating with CO₂ enhanced shale gas recovery is a promising technology to reduce the water consumption and could provide the potential for CO₂ sequestration. Advancing the understanding of complex gas shale reservoir behavior in the presence of multiphase and multicomponent gases (ScCO₂, gaseous CO₂ and CH₄ etc.) via laboratory experiments, theoretical model development and field validation studies is very important. In this paper, the progress of some key scientific problems such as the mechanism of ScCO₂ drilling and completion, the ScCO₂ fracturing technology, the competition adsorption behaviors of CO₂/CH₄ in shale, the coupled multiphase and multicomponent CO₂/CH₄ flow during the CO₂ enhanced shale gas recovery process and the CO₂ sequestration potential in shale formation were discussed. The results indicated that the ScCO₂ jet has a stronger rock erosion ability and requires much lower threshold pressure than water jet. The fracture initiation pressure of ScCO₂ is about 50% lower than that of hydraulic fracturing, and the volume of rock fractured by ScCO₂ is several times larger than that of hydraulic fracturing. Field test shown that the shale gas production rate was significant increased by the ScCO₂-based fracturing technology. Finally, the challenges of the technique will face and the further research is needed in the future is exposed.

1. Introduction

The recoverable reserve of shale gas is approximately 207×10^{12} m³, accounting for 32% of the total natural gas resources of the world (EIA, 2011; Melikoglu, 2014), which plays an important role in world energy supply. The United States is the first country achieved large-scale commercial production of shale gas. Inspired by the shale gas revolution in the US, China is trying to replicate the success of shale gas exploitation. Jiaoshiba shale gas field, which located in southwest China, has becoming the biggest gas field outside North America (Hu et al., 2018; Ma and Xie, 2018). The rapid development of shale gas relies on the breakthrough and development of horizontal drilling and hydraulic fracturing technologies (King, 2010; Rafiee et al., 2012; Nagel et al., 2013; Rutqvist et al., 2015; Wang et al., 2018a; Rahimi-Aghdam et al., 2019; Nguyen-Le and Shin, 2019). Currently,

the most common working fluid used for the commercial shale gas development is slick-water. However, the aqueous-based drilling and fracturing fluids show some notable drawbacks, including but are not limited to: 1) clay minerals are generally distributed in shale gas reservoir, water-based working fluids will induce the hydration of swelling clay, which may damage shale gas formation, and cause the collapse of wellbore and the blockage of gas percolation channel (Dehghanpour et al., 2012; Distefano et al., 2019); 2) hydraulic fracturing consumes large amount of water resources in shale gas development. Limited water availability may restrict shale gas production in water-scarce regions. The fracturing of a typical shale gas well requires 14,000 to 24,000 m³ of water depending on the drilling depth of the well, number of fracturing stages, and length of laterals (Nicot and Scanlon, 2012; Scanlon et al., 2014; Vengosh et al., 2014; Kondash et al., 2018; Zou
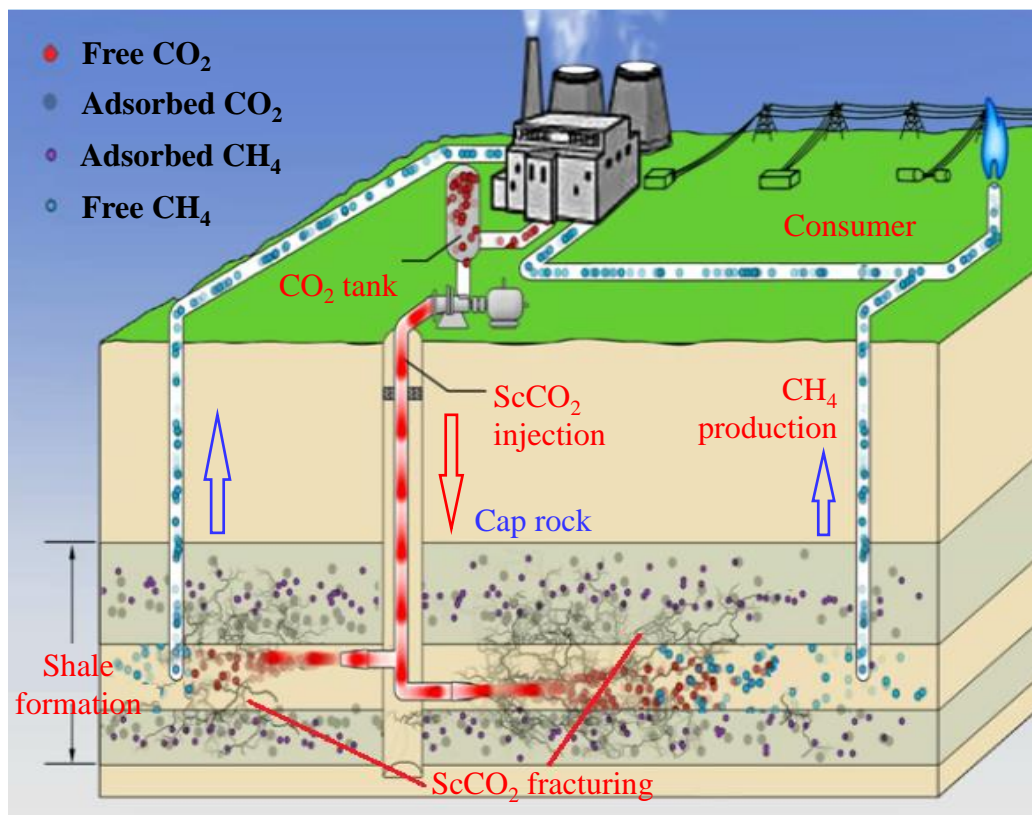
Fig. 1. Schematic diagram of ScCO$_2$ fracturing for enhanced shale gas recovery and CO$_2$ sequestration (developed after Li and Kang, 2018).

et al., 2018). Especially for China, the shale gas reservoirs are located in the area or adjacent area which are short of water resources, the scarcity of water resources is an obvious challenge for shale gas devel-opment in China; 3) in addition to water, the fracturing fluids contain a variety of chemical additives (e.g., friction reducers, thickening agents, gelling agents, crosslinkers, swelling inhibitors, corrosion inhibitors, breakers, biocides, and stabilizers) and proppants, which may have adverse effects on the groundwater and surface water environment (Gregory et al., 2011; Osborn et al., 2011; Estrada Bhamidimarri, 2016; Kondash et al., 2018). To overcome these drawbacks, an increasing number of researchers are exploring less water-intensive or waterless fracturing technologies for the shale gas development.

When the temperature and pressure of CO$_2$ are over the critical points (critical temperature of CO$_2$ T_c = 31.05 °C, critical pressure of CO$_2$ P_c = 7.38 MPa), CO$_2$ will achieve its supercritical state (ScCO$_2$). ScCO$_2$ has some unique and interesting properties, such as low viscosity and high diffu-sivity, which can be used as an ideal non-aqueous drilling and fracturing fluid for shale gas and oil exploitation (Mo et al., 2014; Jia et al., 2019). Compared with aqueous fluids, the unique properties of ScCO$_2$ present more advantages for shale gas development. First, rock breaking with ScCO$_2$ jet has a low threshold pressure and a high rate of penetration compared with water jet. Furthermore, it can induce more complicated fractures due to its low viscosity, enhance shale gas recovery by displacing adsorbed methane in shale, reduce the water footprint, and minimize environmental impacts (Pei

et al., 2015; Zhou et al., 2016; Peng et al., 2017; Zhang et al., 2017a; Jiang et al., 2018). Moreover, ScCO$_2$-based fracturing technology offers the opportunity for CO$_2$ sequestration in shale gas reservoirs (Zhou et al., 2012, 2018a; Middleton et al., 2015).

Based on the above advantages of the ScCO$_2$ in the shale gas development, an innovative idea that integrated the ScCO$_2$ fracturing technology for shale gas recovery and CO$_2$ sequestration was proposed. The main idea of the research is that using ScCO$_2$ to replace the water as drilling and fracturing fluids to enhance the permeability of shale gas reservoir, then utilizing the preferential adsorption behaviors of CO$_2$ over CH$_4$ in shale to enhance the recovery of shale gas, and simultaneously sequestrate CO$_2$ in shale gas formations (Fig. 1). This paper describes the results and accomplishments achieved to date in this field and some of the future activities being considered.

2. Supercritical carbon dioxide as a working fluid for shale gas development

2.1 Shale breaking with supercritical CO$_2$ jet

In the early days, high-pressure water jet technology was widely applied in the well drilling of the oil and gas devel-opment. However, to some extent, the commonly used water jet technology can't match the demands of low cost and high efficiency for drilling. ScCO$_2$, as its unique properties of a gas-like viscosity and a liquid-like density, it can be used to
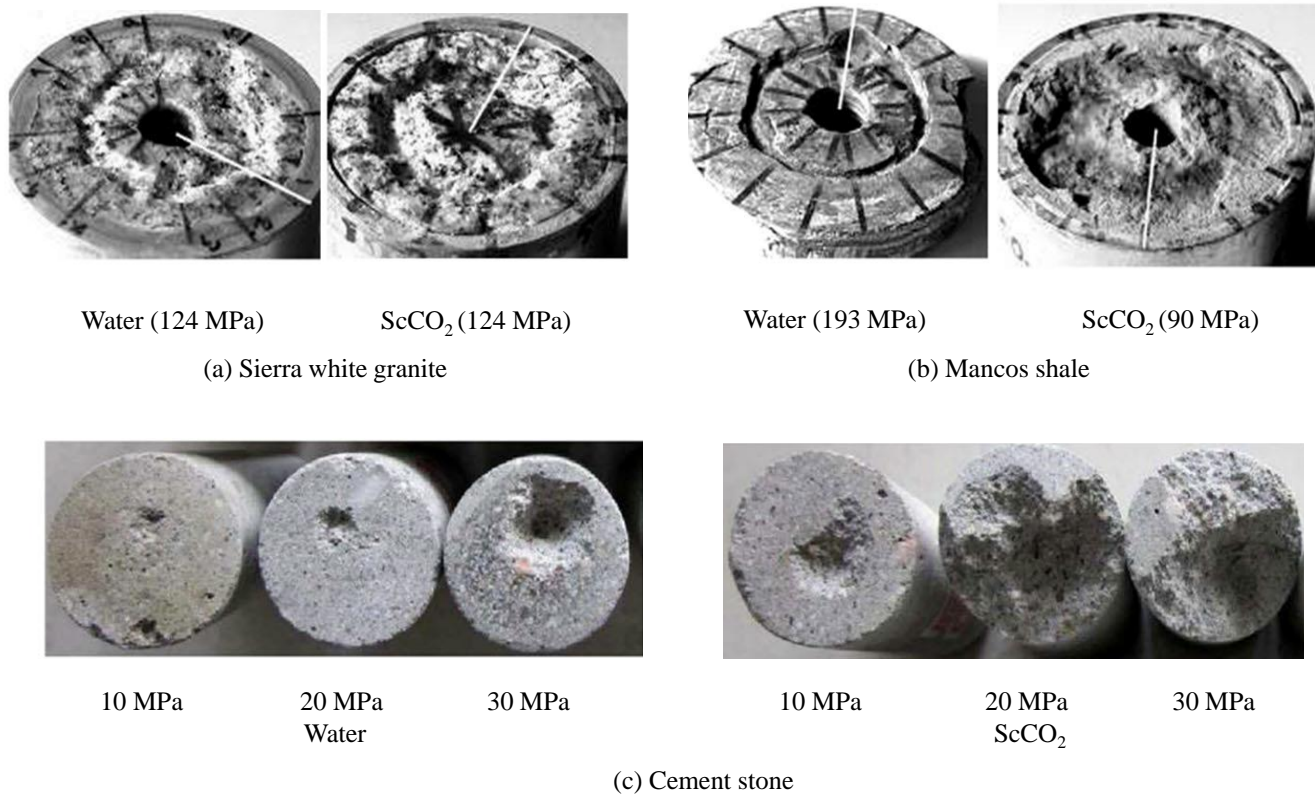
Water (124 MPa) $ScCO_2$ (124 MPa)

(a) Sierra white granite

Water (193 MPa) $ScCO_2$ (90 MPa)

(b) Mancos shale

10 MPa   20 MPa   30 MPa

Water

10 MPa   20 MPa   30 MPa

$ScCO_2$

(c) Cement stone

Fig. 3. Rock-breaking performance between water jet and $ScCO_2$ jet (Kolle, 2000; Li et al., 2018a).
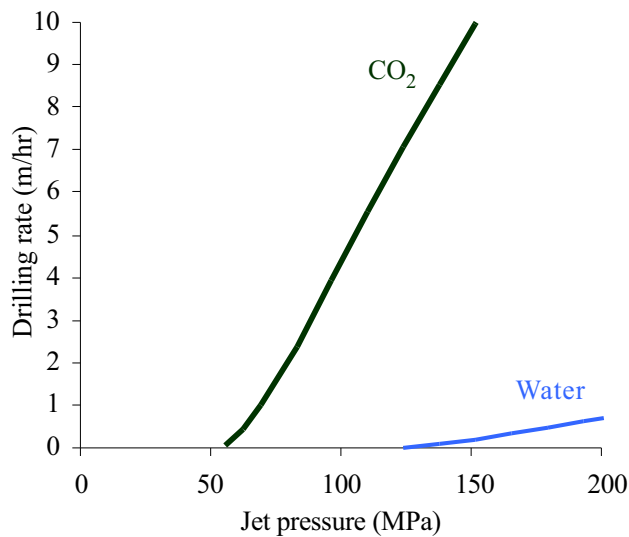

Fig. 2. Projected jet-erosion drilling rates in hard shale (Kolle, 2000).

break rock like water, and could decrease the dissipation of energy from the nozzle to the rock. Moreover, the high diffusivity allows $ScCO_2$ to enter tiny spaces and transmit the fluid static pressure, which is beneficial to improve the rock-erosion efficiency (Du et al., 2012; He et al., 2015, 2016a, 2016b; Song et al., 2016; Cai et al., 2017, 2018, 2019; Huang

et al., 2018b, 2019; Wang et al., 2018a, 2019b). Thus, $ScCO_2$ jet-assisted radial drilling technology is regarded as a potential alternative drilling method as its higher efficiency in rock-erosion efficiency than water jet.

The first research on the rock erosion characteristics of a $ScCO_2$ jet was conducted by Kolle in the late 1990s, stimulated by the demand of improving the drilling efficiency and reducing the working pressure in coiled-tubing drilling (Kolle, 2000). The results indicated that the $ScCO_2$ jet has a stronger rock erosion ability and requires much lower threshold pressure than water jet. The threshold pressure for $ScCO_2$ jet is just 2/3 for water jet when breaking the granite and even less than half for water jet when breaking the shale. The specific energies for eroding granite and Mancos Shale using $ScCO_2$ jets are less than 50% and only 3% those of water jets, respectively. The rate of penetration in Mancos shale applying a $ScCO_2$ jet was 3.3 times that observed while drilling with a water jet (Fig. 2). The results have also been confirmed by other researchers by using different rocks (Fig. 3). As can be seen from Fig. 3, $ScCO_2$ appears to be more efficient than water jet in slim-hole radial drilling and it has a lower rock breaking threshold pressure than that of water jet (Kolle, 2000; Li et al., 2018a).

With the rapid development of shale gas in china, some exploratory studies on the mechanism of shale breaking by supercritical CO_2 jet were conducted (Wang et al., 2012, 2015a). He et al. (2016a) conducted rock erosion experiments
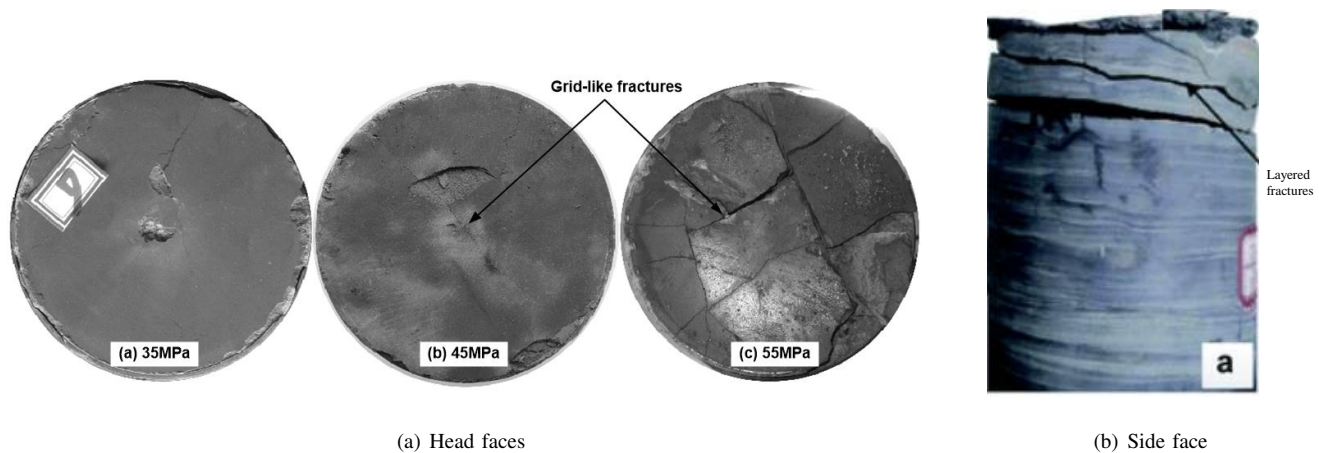
(a) Head faces

(b) Side face

Fig. 4. Shale-cores impacted by $ScCO_2$ jet (Huang et al., 2018a).

using $ScCO_2$ jets on different rocks and made subsequent in-depth SEM observation and analyses. They demonstrated that a $ScCO_2$ jet erodes rock substances mainly in the brittle tensile failure mechanism and facilitates the rock to be further broken, accompanied with the shear failure mechanism in particular locations of the erosion hole. Huang et al. (2018a) studied the microstructure changes between the original shale sample and the eroded sample after $ScCO_2$ jet by using the methods of CT, SEM/EDX, XRD and XRF. The results illustrated that the surface of shale sample shot by a $ScCO_2$ jet shows a grid-like breakage, and the sample was broken into layers with a large volume overall (Fig. 4). The erosion of shale mineral induced by the $ScCO_2$ jet impingement can also change the microstructure of shale and then reduce its mechanical strength.

Through theoretical analysis and numerical simulation, some research explored the properties of the $ScCO_2$ jet flow field, and the influencing factors on the flow field of the $ScCO_2$ jet (Hu et al., 2016; Zhou et al., 2017a; Huang et al., 2018b). The results indicated that the velocity and the pressure of the $ScCO_2$ jet could be converted to each other, and the $ScCO_2$ jet has a stronger impact pressure and a higher velocity than those of the water jet under the same conditions, the maximum velocity and the impact pressure of the $ScCO_2$ jet increase with the increase of the nozzle pressure drop, $ScCO_2$ impacting jet has a more obvious thermal effect on the wall without any phenomena of CO_2 freezing and blocking nozzle.

However, though theoretical, experimental and numerical simulation studies were conducted to disclose the main factors, including the jet pressure, jet temperature, confining pressure, jet distance, rotary speed of core samples and jet time, which influence the rock-breaking performance and efficiency (Hu et al., 2016; Shi et al., 2016; Zhou et al., 2017a; Huang et al., 2018b; Li et al., 2018b; Sun et al., 2018a), further works on the wellbore pressure control theory, the rock-erosion rules and the cutting-carrying ability of supercritical carbon dioxide drilling especially at horizontal section are needed to understand the mechanisms of shale breaking with $ScCO_2$ jet for promoting

the engineering application of this technology.

2.2 Mechanism of supercritical carbon dioxide fracturing in shale gas reservoir

As most shale formations in China have high clay contents and low or ultra-low permeability (Xiong et al., 2015; Zhou et al., 2017b), the water-based fracturing technology will cause clays swelling, which may lock the gas channels and further decrease the gas production. As a non-aqueous fracturing fluid, $ScCO_2$-based fracturing technology has shown a promising application in shale gas development (Zhou et al., 2016; Zhang et al., 2017a).

Experiments has been conducted to reveal the mechanism of $ScCO_2$ fracturing in shale (Zhou et al., 2016; Zhang et al., 2017a; Jia et al., 2018a; Jiang et al., 2018; Zhao et al., 2018; Zhou et al., 2018b, 2019b; Zhang et al., 2019). The results were indicated that the $ScCO_2$ fracturing induced more complicated and rough fractures than that of induced by hydraulic fracturing, thus $ScCO_2$ fracturing are more likely to form complex fracture networks. The volume of rock fractured by $ScCO_2$ is several times larger than that of hydraulic fracturing. Compared with hydraulic fracturing and liquid CO_2 (L-CO_2) fracturing, the fracture initiation pressure of $ScCO_2$ is the lowest, which was about 15% lower than that of L-CO_2, and almost 50% lower than that of hydraulic fracturing (Fig. 5) (Wang et al., 2017; Zhang et al., 2017a). The acoustic emission (AE) sources of the Sc- and L-CO_2 injections tend to distribute in a larger area than those of water injection, and furthermore, $ScCO_2$ tended to generate cracks extending more three dimensionally rather than along a flat plane than L-CO_2 (Ishida et al., 2012, 2016; Zhang et al., 2017a). The results are also consistent with the results of the fracturing experiments conducted by using cubic granite blocks (Ishida et al., 2012; Inui et al., 2014; Chen et al., 2015b).

The fracture extension model with $ScCO_2$ appeared to be different from that of water (Ishida et al., 2012; Zhang et
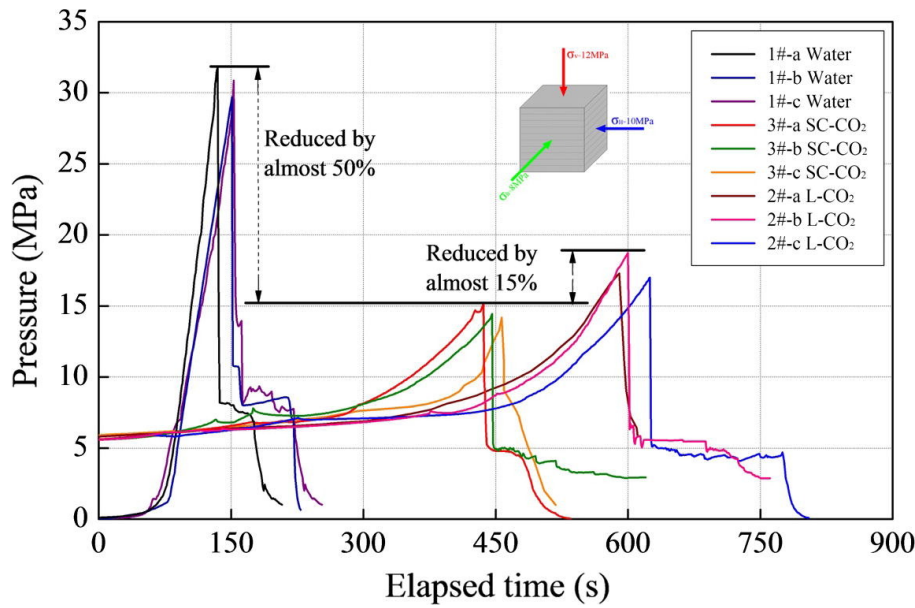
Fig. 5. The fracture initiation pressures for water, L-CO_2 and ScCO_2 fracturing in shale (Zhang et al., 2017a).
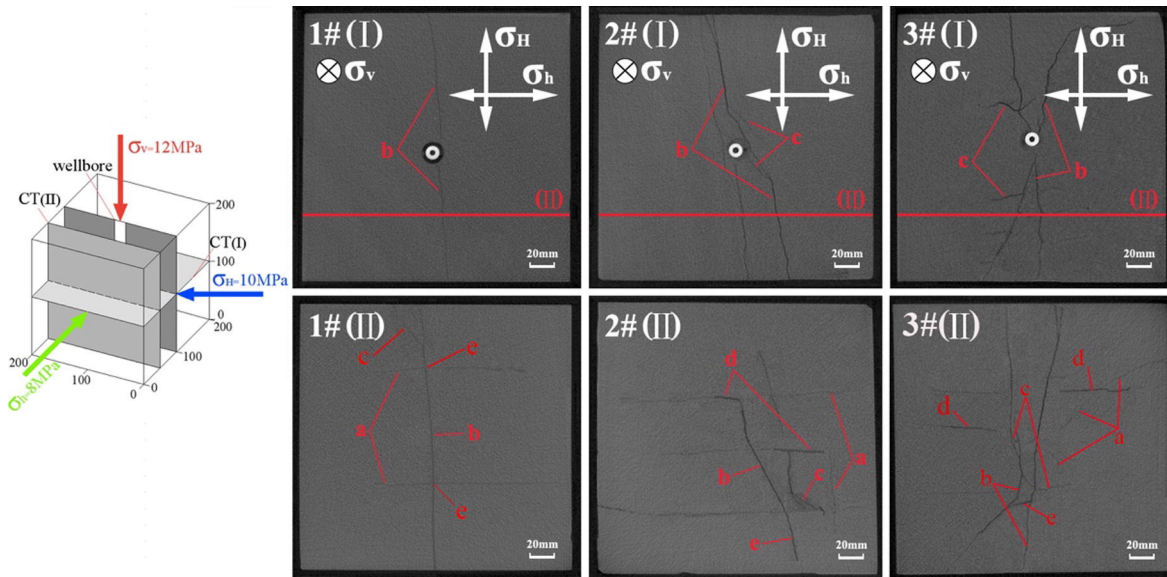

Fig. 6. CT scanning images of specimens using different fracturing fluids. 1# (with water), 2# (L-CO_2), 3# (ScCO_2). (I) images recorded from the scan CT (I) plane, (II) vertical images recorded from the CT (II) plane (Zhang et al., 2017a).

al., 2017). ScCO_2-induced fractures are dominated by shear fractures, including tensile fractures. Fracture extension with shear dominant fractures, which occurred during the CO_2 injection, is likely sensitive to defects, such as bedding weak planes, in a core. The difference in the fracturing modes of ScCO_2 and water seems to be significantly affected by the viscosity. Unlike water, ScCO_2 has a high diffusivity, low viscosity, and low surface tension. It thus can penetrate into micro defects and even smaller pore spaces of the shale samples. Moreover, when the pressure of CO_2 drops as the fractures extending during the fracturing process, ScCO_2 could suddenly change to the gaseous state. As the compressibility of the gas state is much larger than that of the supercritical state, this phase transition could lead to the expansion of ScCO_2 and

induce further fracturing, which is beneficial to the fractures extension and could create more fractures in all directions. Thus, compared to the conventional slick-water fracturing, ScCO_2 injection induces more widely extended fractures with multiple branches (Fig. 6) (Zhang et al., 2017a).

The experimental and numerical results commonly indicate that significant fluid permeation during ScCO_2 fracturing is a primary reason for its lower breakdown pressure and more distributed fractures compared with hydraulic fracturing (Li et al., 2016; Zhang et al., 2017a; Ha et al., 2018; Jia et al., 2018a; Jun et al., 2018; Wang et al., 2018b; Wang et al., 2019a). ScCO_2 may also more effectively fracture shale rock due to coupled compressibility-thermal shock effects. Specifically, strong Joule-Thompson cooling effect may enhance fracturing

due to thermal stress created as CO_2 expands into a new fracture volume and cools the crack tip (Middleton et al., 2014).

For shale gas reservoirs, fracturing often aims to create propped fractures with a certain flow conductivity, the distribution of proppant is the key factor that influences the flow conductivity of the fracture. Thus, the proppant carrying capacity of $ScCO_2$ is a key factor should be considered for the engineering application of $ScCO_2$ fracturing in unconventional gas reservoir development (Song et al., 2018a; Sun et al., 2018b). However, the low viscosity of $ScCO_2$ in reservoir conditions prevents effective transport of proppants deep into stimulated fractures, and the volume of injected proppant by $ScCO_2$ during the fracturing is limited (Wang et al., 2014; Hou et al., 2015, 2017a, 2017b; Dai et al., 2018; Du et al., 2018; Li et al., 2019). To overcome this limitation, two general strategies are commonly pursued: Thickening CO_2 and foaming CO_2 (Ribeiro et al., 2017; Jing et al., 2019). In future, developing an effective, economical and environmentally friendly thickener for $ScCO_2$ is needed to enhance its proppant carrying capacity. For foaming CO_2, as conventional foams still contain significant fractions of water by volume (one tenth to one quarter) that can contribute to formation damage, ultra-dry foams containing less water should be developed.

2.3 Competition adsorption behaviors of CO_2/CH_4 in shale

Since a large proportion of gas in shale reservoirs is stored as an adsorbed state, competitive adsorption behaviors involving CO_2 and CH_4 are of key importance for the optimal of CO_2-enhanced shale gas recovery and CO_2 sequestration processes (Sun et al., 2013; Xu et al., 2017; Myshakin et al., 2018; Zhou et al., 2018a). Extensive investigate efforts have been conducted to study the adsorption of CH_4 and CO_2 on shales under single gas environment and binary gas environment, and the influence of different affecting factors, such as total organic carbon (TOC) content, organic matter type, thermal maturity, clay mineral content, and pore structure on the selective behavior of CH_4 and CO_2 adsorption on shales were also determined (Cancino et al., 2017; Gu et al., 2017; Wang et al., 2018c, 2018d; Huang et al., 2018c, 2019; Zhou et al., 2018a). The main results indicated that the adsorption capacity of CO_2 on shale is always greater than that of CH_4, and the adsorption ratios of CO_2 to CH_4 (α_{CO_2/CH_4}) show widely varying ranges for different shales. Nuttall et al. (2005) observed that CO_2 is adsorbed approximately 5 times more than that of CH_4 for Devonian black shales. Weniger et al. (2010) reported α_{CO_2/CH_4} varied between 1.9 and 6.9 for several carbonaceous shale samples from Paraná Basin, Brazil. Similar study of preferential adsorption was conducted by Kang et al. (2011) on two Barnett shale samples from USA. It was found that CO_2 adsorbed 5-10 times more than CH_4. The CO_2 adsorptive capacity for Barnett, Eagle Ford, Marcellus and Montney shales from USA was measured to be 2-3 times higher than that of CH_4 (Heller et al., 2014a). For Sichuan Basin shale, the value of α_{CO_2/CH_4} ranges from 2.5 to

6.9 (Duan et al., 2016; Qi et al., 2018). Heller et al. (2014a) obtained that CO_2 has approximately 2-3 times the adsorptive capacity of CH_4 in both the pure mineral constituents and actual shale samples. Gu et al. (2017) hold that shale with high clay contents and more micropores is more likely has a greater α_{CO_2/CH_4}. Huang et al. (2018c) obtained that the adsorption ratios of α_{CO_2/CH_4} are in the order of kerogen IA < IIA < IIIA for different organic types. For CO_2/CH_4 mixtures adsorption in shale, CO_2 also preferentially adsorbs over CH_4 in the competitive adsorption process (Luo et al., 2015; Duan et al., 2016; Niu et al., 2018; Wang et al., 2018d). The competition adsorption behaviors of CO_2/CH_4 are influenced by many factors, such as the reservoir pressure and temperature, pore structure and mineral composition of shale (Luo et al., 2015; Hong et al., 2016; Gu et al., 2017; Psarras et al., 2017; Zhou et al., 2019a). As the many affecting factors mentioned above contribute to the variability of α_{CO_2/CH_4} in different shales, thus, it is important to study this on a case by case basis.

The gas retention capacity of a shale gas reservoir under simulated geological temperature and pressure conditions can be estimated from an adsorption isotherm. Finding an optimized adsorption model to estimate the true adsorbed quantity of CH_4 and CO_2 in shale at reservoir conditions is fundamental for estimating the CO_2 storage capacity and analyzing the shale gas production. To date, many gas adsorption isotherm models have been developed to describe the experimental adsorption data. For single gas adsorption, these include the Langmuir, Dual-Langmuir, Dubinin-Radushkevich (D-R), Dubinin-Astakhov (D-A), BET, Lattice Density Functional Theory (LDFT) and Ono-Kondo Models (Charoensuppanimit et al., 2016; Tang et al., 2016, 2017a, 2017b; Xiong et al., 2017; Chen et al., 2018b; Singh and Cai, 2018; Song et al., 2018b; Zhou et al., 2019a). Whereas for multicomponent gas adsorption their combination with the extended Langmuir equation, multicomponent potential theory of adsorption (MPTA), ideal adsorbed solution (IAS) theory have been applied (Ambrose et al., 2011; Fathi and Akkutlu, 2014; Wang et al., 2015b; Ren et al., 2017; Kulga and Ertekin, 2018). Among these models, Langmuir isotherm model is the most common model used to describe adsorption of methane and CO_2 on shales, its relatively simple form allows for direct implementation in reservoir simulators describing enhanced shale gas recovery (ESGR) processes. However, some exceptional trends have also been reported. Bi et al. (2017) hold that both Langmuir and Ono-Kondo models exhibit excellent correlation with the experimental adsorption data of CH_4, and the Ono-Kondo model appears to be more reliable for supercritical adsorption. Rexer et al. (2013) observed that the modified D-R model is superior to the Langmuir model for supercritical CH_4 adsorption. Wang et al. (2016) observed that both D-A and Langmuir models performed well CH_4 adsorption on organic-rich shale samples, while the BET model show a poor performance for CH_4 adsorption on shale. All these studies indicated that the modeling exercise should be continued to evaluate the relative accuracy of various models in predicting the adsorption behavior of shales, especially for supercritical CO_2 and multi-component gaseous systems in shale.

Overall, majority of the studies focus adsorption for pure

gas components, while on mixed gas adsorption studies in shale are rare, further work is needed to perform rigorous laboratory test to obtain more multicomponent adsorption data, and develop more rigorous, theory based, thermodynamically consistent adsorption model to improve the capability in predicting multi-component adsorption behavior in shale (CH_4, gaseous CO_2 and $ScCO_2$). In addition, in most of the shale gas reservoirs, carbon dioxide exists in supercritical condition and more studies should be addressed on $ScCO_2$ adsorption in shale.

2.4 CO_2-shale interaction

2.4.1 The CO_2-shale interaction on the physical and chemical properties of shale

The injected CO_2 will interact with shale components (i.e. clays, organic matter) and affect rock properties and fluid transports through chemical alteration, matrix swelling/shrinkage, and related geo-mechanical effects. As changes in rock properties will impact both CO_2 sequestration and hydraulic fracturing, it is imperative to increase our understanding of the CO_2-shale interactions.

Many characterization methods such as scanning electron microscopy (SEM), X-ray diffraction (XRD) analysis, X-ray fluorescence (XRF) spectrometer, low-pressure gas (N_2 and CO_2) adsorption, (ICP-MS), Fourier transform infrared (FTIR) spectroscopy and nuclear magnetic resonance (NMR) technology were used to investigate the effects of CO_2-shale interactions on the microstructure and chemical properties of shale (Jiang et al., 2016; Yin et al., 2016; Ao et al., 2017; Pan et al., 2018a; Hui et al., 2019). The results indicated that CO_2-shale interactions can alter the microstructure and geochemical properties of shale, and this alteration is related to the temperature, pressure, phase states of CO_2 and the type of shale (Qin et al., 2017; Zhou et al., 2017b; Pan et al., 2018a; Goodman et al., 2019).

$ScCO_2$-shale interactions had a more significant effect on the pore structure of shale than that of $SubCO_2$-shale interaction, which was attributed to the greater dissolution and expansion effect as well as the extraction ability associated with supercritical CO_2 (Yin et al., 2016; Zhou et al., 2017b; Pan et al., 2018b; Lu et al., 2019). Rezaee et al. (2017) observed that there is a reduction in the capillary threshold pressures and an increase in pore volume for most of the shale samples exposed to $ScCO_2$. Pan et al. (2018a, 2018b) found that the $SubCO_2$ and $ScCO_2$ exposures had different influences on the micro-, meso- and macropore structure of marine and terrestrial shales. Specifically, the specific surface area (SSA), pore size distribution (PSD) as well as the porosity of the $SubCO_2$-treated shale samples were lower than those of the raw samples. However, $ScCO_2$-shales interactions created a more significant influence on the pore structure compared to those of subcritical CO_2-shale interactions, and it should be noted that the variation trend of pore structure parameters for different types of shale samples was quite different, which was related to the huge discrepancies in terms of mineralogy and geochemical properties between them. For marine shale

samples, the pore surface area and pore volume obviously decreased after a relatively short period of $ScCO_2$ treatment, whereas an opposite trend was observed in a terrestrial sample after long-term $ScCO_2$ treatment. In addition, an obvious decrease in fractal dimensions for marine Longmaxi sample was also observed after $ScCO_2$ exposure, reflecting the degree of pore surface roughness, and pore structure complexity were reduced, whereas the terrestrial sample exhibited an opposite trend. The changes in the pore structure of shale associated with $ScCO_2$-shale interactions could be interpreted by two mechanisms: The dissolution effect of $ScCO_2$, which enlarged the pore size; and the CO_2 adsorption-induced swelling, which narrowed the pores. The CO_2-shale interactions induced the changes to the pore structure in the shale may modify the flow pattern of the gas in the process CO_2 enhanced shale gas recovery (CO_2-ESGR), which need further research in the future.

CO_2-shale interactions also altered the chemical properties of shale, chemical reactions include dissolution and precipitation of several authigenic minerals such as kaolinite, natrojarosite, silica and gypsum. Sanguinito et al. (2018) found that carbonate formation and dissolution occurs in shale exposed to dry CO_2, and etching and pitting occur, with minor calcite precipitation along the surface of the shale sample. Yin et al. (2016) observed that montmorillonite, kaolinite and calcite content in shale sample decreases due to the dissolution induced by $ScCO_2$. Ao et al. (2017) observed that the mineral content of all the shale minerals except quartz decreased after $ScCO_2$ exposure. Luo et al. (2019) measured the element mobilization and pore structure before and after the $ScCO_2$-water-shale reaction using the shale samples of Qaidam Basin and Ordos Basin in China. The results indicated that the major elements, including Ca, Mg, Na, K, and Al, exhibit varying degrees of mobilization after the interactions because of dissolution of carbonate and silicate minerals in shale samples. Compared with the major elements, trace elements have a lower mobility, quantified as $< 13.97\%$. However, the trace elements Sr, Zn, Co and Ba that mainly exist in carbonate and sulfide minerals are more easily mobilized than other trace elements. Thus, under the conditions of $ScCO_2$ fracturing or CO_2 sequestration in shale gas reservoirs, the underground water below the operating regions must be monitored because trace elements such as Sr, Zn, Co, and Ba can be mobilized and potentially contaminate groundwater.

As the CO_2-shale interactions has different influence on the different types of shale samples, and the reservoir temperatures and pressures also have significant impacts on the $ScCO_2$-shale interactions. Thus, it is necessary to study shale-CO_2 interactions on a case by case basis. Furthermore, the interactions of CO_2-shale are also time dependent, then further research on the reaction kinetics of shale-CO_2 in different time scales is also needed in future.

2.4.2 The CO_2 saturation on the mechanical properties of shale

The CO_2-shale interactions induced microstructure and mineral composition alteration may have significant influence on the mechanical properties of shale, which should be crit-
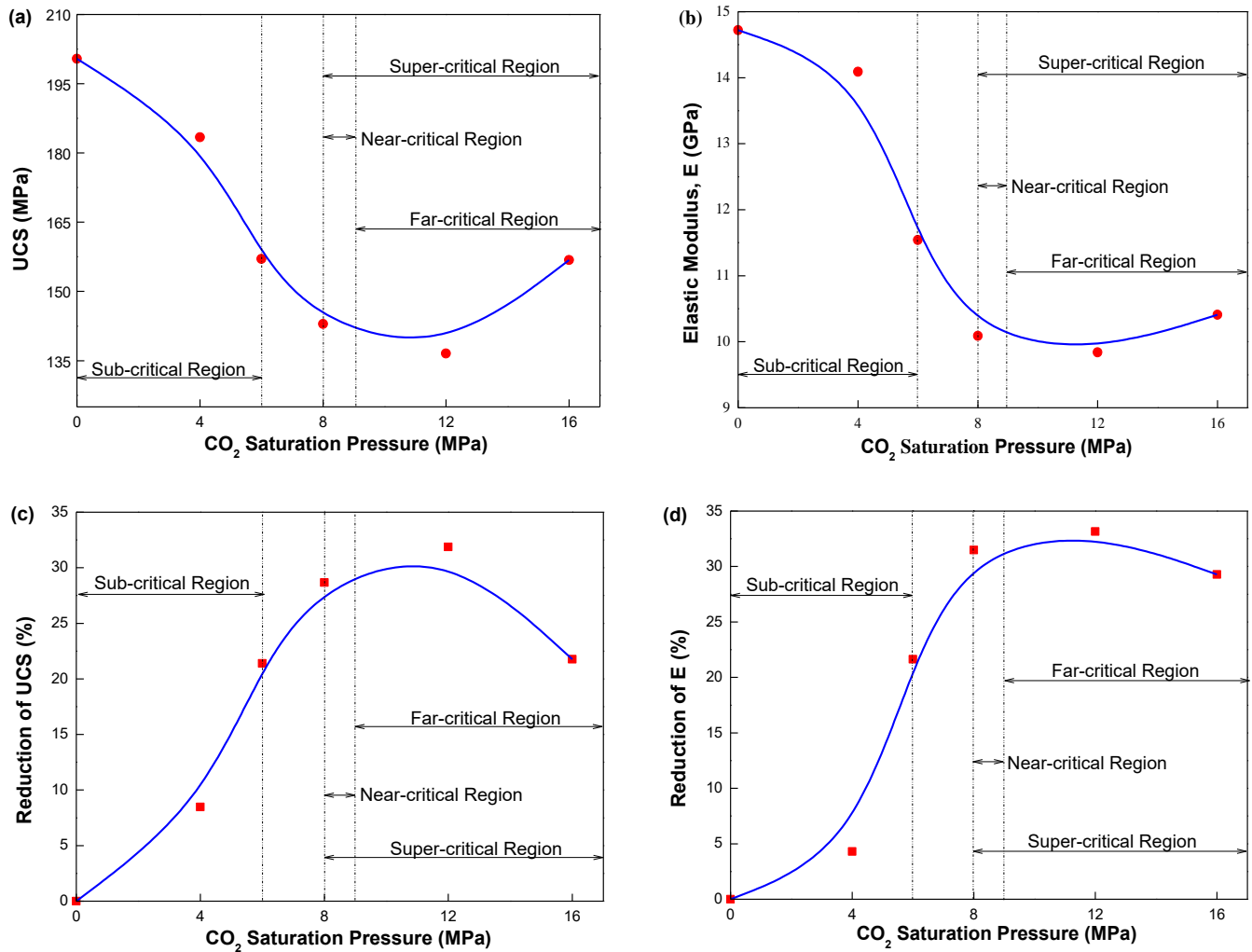
Fig. 7. Effect of CO_2 adsorption pressure and phase change on UCS and Young's modulus of shale (Yin et al., 2017).

ically evaluated to enhance the efficiency of CO_2-ESGR and CO_2 sequestration processes, and mitigate associated hazards. Many laboratory studies testing the interaction of shale between different saturation fluids (water, $SubCO_2$, $ScCO_2$) on the mechanical properties of shale. Both of sub-/super-critical CO_2 saturation weaken the strength and increase the ductility of the shale, as the uniaxial compressive strength (UCS) and Young's modulus (E) were decreased after CO_2 saturation (Yin et al., 2017; Zhang et al., 2017b; Lyu et al., 2018a, 2018b, 2019; Feng et al., 2019; Lu et al., 2019). However, $ScCO_2$ saturation causes a greater reduction of shale's mechanical properties than that of $subCO_2$, which in-dicated that the influence of CO_2 saturation on mechanics of shales is also highly depending on the saturation pressure and the phase state of CO_2 (Yin et al., 2017; Lu et al., 2019). Yin et al. (2017) observed that $ScCO_2$ saturation caused a reduction of 33.89% in UCS of organic-rich shales, which is higher than that of 22.86% caused by $SubCO_2$ saturation. The reduction in E of organic-rich shales caused by $ScCO_2$ saturation is 33.97%, which is higher than that of 23.10% caused by $SubCO_2$ satura-tion (Fig. 7). Lyu et al. (2018b) observed that the UCS and E of shale decrease with the increase of saturation time, and $ScCO_2$

saturation creates more AE energy than $SubCO_2$ saturation (Fig. 8). The macroscopic mechanical properties alteration of shale caused by CO_2 saturation can be interpreted by the microscopic changes induced by CO_2-shale interactions, as previously mentioned. The discrepancies of mechanical behavior of shale caused by $SubCO_2$ and $ScCO_2$ saturation is also consistent with the microstructure alteration of shale caused by $SubCO_2$ and $ScCO_2$. In addition to the adsorption-induced swelling effect, the extraction and dissolution effects of $ScCO_2$ induced microstructural alterations could cause more additional damages, which caused a greater weaken of shale.

The results of the experimental investigation provide per-suasive evidence to conclude the fact that CO_2 interaction causes significant mechanical degradation in shale. However, the degree of strength reduction is influenced by multiple factors, including geo-environment characteristics of shale formations, CO_2 phase, adsorption pressure, interaction time, etc. The micro-cracks caused by the CO_2 adsorption induced heterogeneous swelling and chemical interactions, contribution to the overall mechanical degradation in the shale mass. For in-situ reservoir environment, during the fracking or sequestrating process, CO_2 will form carbonic acid when meeting water or
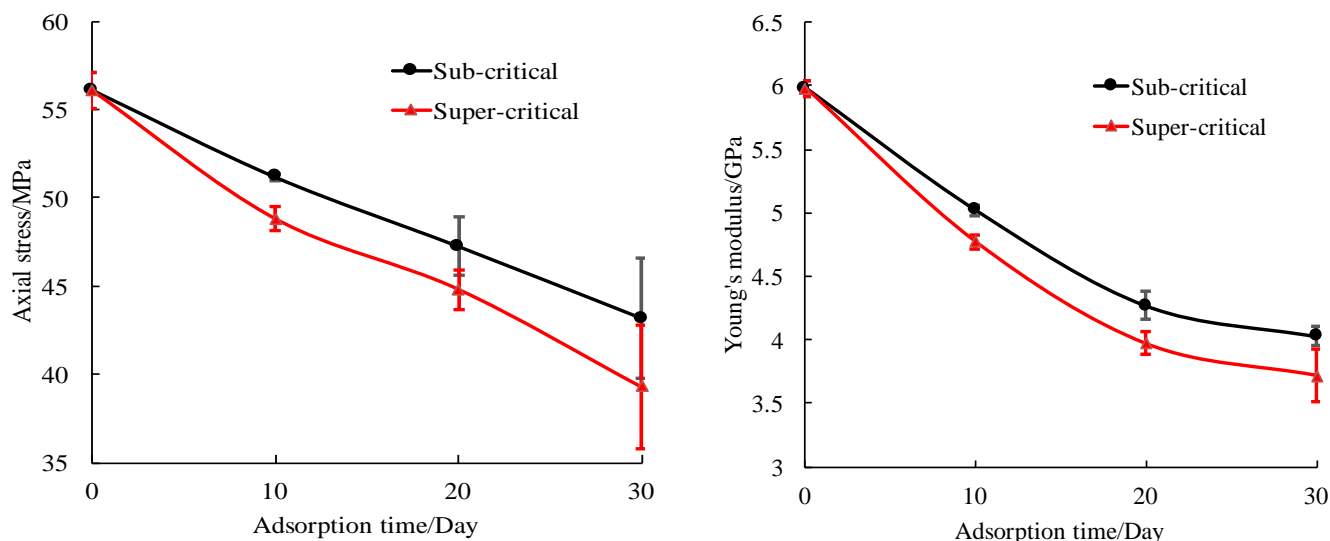
Fig. 8. Effect of CO_2 adsorption time on UCS and Young's modulus of shale (Lyu et al., 2018b).

brines and dissolving into it, which leads to the dissolution and precipitation of minerals. Thus, more attentions are needed to focus on the effect of CO_2-brine-rock interactions on shale samples' mechanical properties (Lyu et al., 2016, 2018a; Zhang et al., 2017b). In addition, the CO_2-shale reaction in reservoir condition covers a long-term timescale, thus the influence of the lon-term shale-CO_2 interactions induced strength alterations should be investigated more rigorously. Moreover, the risk of the strength weakening associated with CO_2-shale interaction on the borehole stability of horizontal wells, and the collapse of the induced fractures should be evaluated. Finally, shale is an extremely heterogeneous and anisotropic material, the mechanical alteration can be varied, thus should be evaluated targeting the specific reservoir characteristics, prior to implementation of CO_2-ESGR projects.

2.5 Gas flow in shale during the process of CO_2-ESGR

The gas flow in shale gas reservoirs is controlled by the permeability of shale, during the CO_2-ESGR process, the permeability of shale gas reservoir is influenced by multiple factors, including geo-stress, pressure, temperature, Klinkenberg effect, CO_2/CH_4 competition adsorption induced differential swelling, CO_2-shale interaction induced damage and fracture (Bhandari et al., 2015; Moghaddam and Jamiolahmady, 2016; Zhou et al., 2016; Li et al., 2017; Wu et al., 2017; Yang et al., 2017; Chen et al., 2019; Lan et al., 2019).

During the CO_2-ESGR process, with the injection of CO_2, the variation of gas pressure will induce the change in geo-stresses, then caused the changes of permeability in shale. The impacts of effective stress on the gas permeability have been studied extensively in the laboratory. For the low effective stress range, an exponential decrease trend of shale can be observed between the permeability and effective stress, the permeability of organic-rich shale decreases rapidly with the increased effective stress especially for the shales with

permeability less than 1 μD (Heller et al., 2014b; Gutierrez et al., 2015; Pan et al., 2015; Moghadam and Chalaturnyk, 2016; Zhou et al., 2016). While at high effective stress range, the gas permeability change behavior shows a two-stage characteristic and nonlinearly decreasing trend with the increase of effective stress, the permeabilities of the intact and fractured shale samples decreased rapidly at low effective stress and decrease slowly at high effective stress at the semi-log plot (Chen et al., 2019). During the CO_2 injection, the effective stress will change with the variation of injection pressure, thus the influence of injection regime and the stress path on the permeability is also should be considered in further research.

In addition, the shale matrix swelling or shrinkage is will also impact on the dynamic evolution of gas flow in shale. It is well-known that the adsorption of gases as CO_2 and CH_4 can cause swelling of shale with decreasing void volume in cleats and fracture networks, which may have a significant impact on gas transport in shales (Lu et al., 2016; Chen et al., 2018a). The amount of shale swelling varies with multiple factors, including the adsorbing gas type, pressure, temperature and the phase state of CO_2 (Fig. 9). Heller et al. (2014b) measured the swelling of pure minerals of gas shale, including carbon, illite and kaolinite, and investigated the relationship between the swelling of pure mineral and the amount of gas adsorption. Chen et al. (2015a) investigated the deformation of shale in Helium and CH_4 at constant confining pressure and different gas pressures, the results indicated that the adsorption induced shale swelling strain shows a Langmuir-like relationship with pressure and is proportional to the amount of methane adsorbed. Miedzińska and Lutyński (2018) measured the CO_2-CH_4 adsorption induced swelling of gas shales, the results indicated that swelling of shale in case of CO_2 adsorption was greater than in the case of CH_4 adsorption, and the swelling is also related to the mineral composition of shale, more swelling of the organic matter than of the clay matrix is occurred. Lu et al. (2016) measure CO_2-induced swelling in shale samples at temperatures between
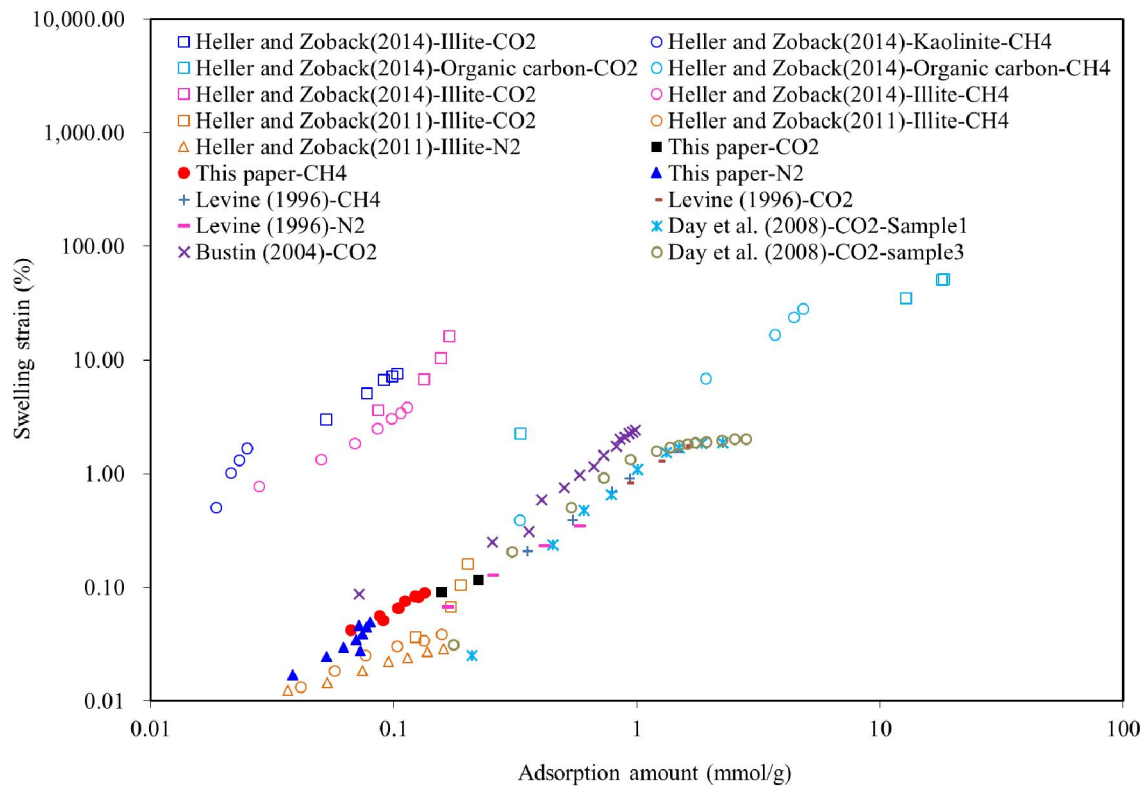
Fig. 9. Relationship between adsorption-induced swelling and the absolute adsorption amount in different types of gases (modified from Chen et al., 2018a).
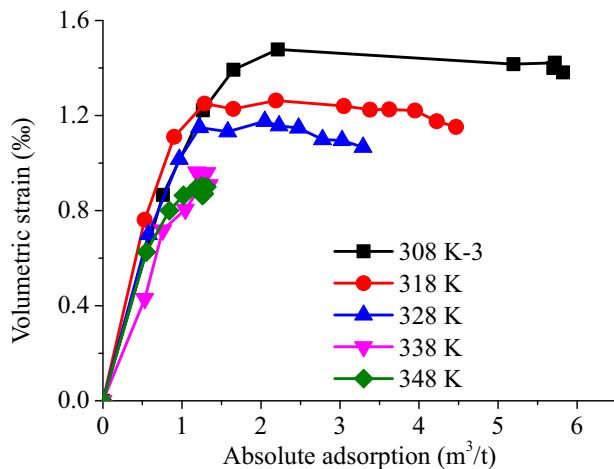

Fig. 10. Influence of adsorbed amount and the temperature on CO_2 induced shale swelling (Lu et al., 2016).

308 and 348 K and pressures up to 15 MPa, which covers the pressure range from subcritical to supercritical CO_2. The results indicated that the swelling of shale is related to the temperature, gas pressure and phase of CO_2, with increasing CO_2 pressure, the swelling of shale samples initially increases and then lessens, and the swelling of shale can be described well by a simplified local-density model. With increasing CO_2 temperature, the maximum swelling of the shale gradually decreases (Fig. 10). In addition, shale exhibited anisotropic swelling in response to CO_2 injection, with the swelling strains

always being less in the direction parallel to the bedding plane (Lu et al., 2016; Pluymakers et al., 2018). Furthermore, the water saturation inside the shale matrix may influence the swelling effect of CO_2-shale matrix interaction, thus, it should be considered at the real reservoir conditions as well.

All these studies were focused on the final strain at the adsorption equilibrium, however, gases are not at adsorption equilibrium during production or CO_2 injection. Based on this, Chen et al. (2018a) investigated the kinetic swelling of organic-rich shale in different gases (CO_2, CH_4 and N_2), they found that the shale swelling rate and the gas uptake rate show a linear relationship and both are affected by gas type and phase state of CO_2, adsorption induced swelling of shale are successively increased in order of N_2, CH_4 and CO_2 (Fig. 11). The phase change of CO_2 is also resulting in the change of kinetic swelling rate. Moreover, the anisotropic swelling behavior is also observed, and the anisotropy ratio is related to the adsorbing gas type as well, with the anisotropy ratio for shale swelling decreases in the order of He, N_2, CH_4 and CO_2. In the CO_2-ESGR process, the adsorption induced swelling may change the porosity of shale, then induce the change of the permeability of shale, the phase change of CO_2 will lead different variation characteristics of permeability in shale reservoir, as CO_2 adsorption induced swelling is dependent to the phase state of CO_2. Furthermore, the adsorption induced swelling may also influence the gas flow mechanism in shale. As the pore size distribution of shale changed by adsorption, the Knudsen number and the Klinkenberg coefficient will
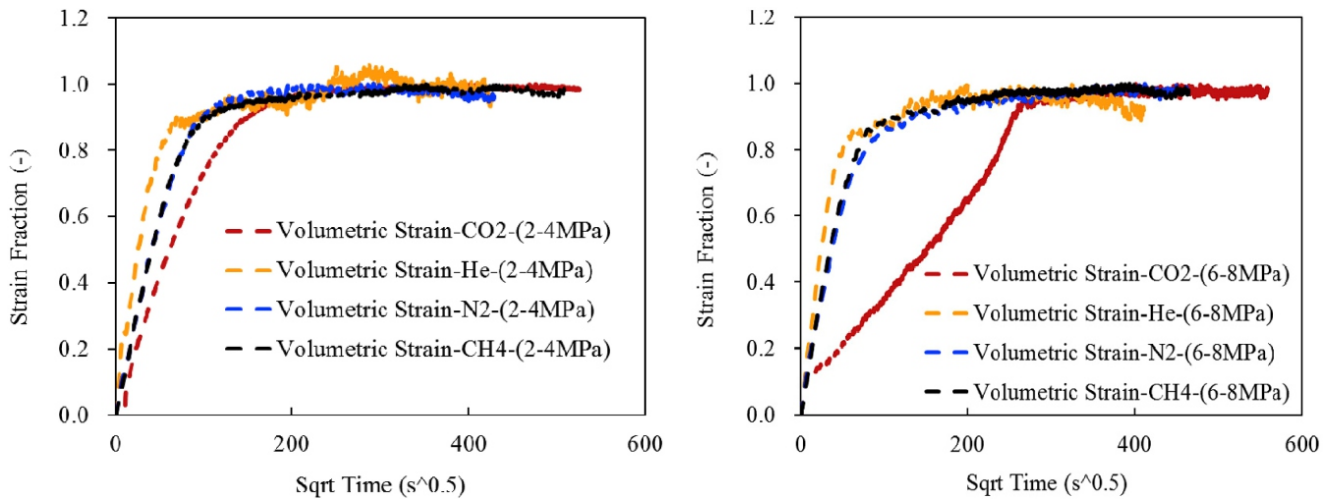
Fig. 11. Evolution of volumetric strain fraction with time (Chen et al., 2018a).

be changed, thus, the gas flow behavior or surface diffusion behavior is varied with the adsorption (Cui et al., 2009; Jia et al., 2018b, 2018c).

Temperature variation is also an important parameter which may influence the shale permeability at a particular stress state (Perera et al., 2012). Adsorption and its consequent adsorption induced swelling, decrease at elevated temperatures. Reduction of swelling effect lowers the pore volume changes and increases the permeability. The temperature difference between the injected CO_2 and shale gas reservoir may induce thermo-mechanical effects in shale. If the temperature difference is significant then it can induce thermal stresses greater than fracture strength of shales. The thermally induced fractures can therefore increase the permeability significantly.

The interaction of $ScCO_2$-shale induced physical and structural changes is another important factor which has significant influence on gas flow in the process of CO_2-ESGR. First, the extraction and dissolution effects of $ScCO_2$ will induce damage and secondary fracture on shale, which is beneficial to enhance the permeability of shale. Second, the $ScCO_2$-shale interaction induced alteration of mechanical properties in shale will change the stress sensitivity of shale, which also has a significant impact on the permeability of shale (Jia et al., 2018a). Moreover, chemical reaction of CO_2-rich aqueous fluids may increase the permeability of fractured shale due to the dissolution effects. Thus, the permeability of shale is competitively controlled by shale swelling, mineral dissolution and chemical reaction effects. The combined effects on shale permeability variation is still not clear, comprehensive and systematic research studies need to be carried out to fully appreciate these influences on permeability changes of shale during the CO_2-ESGR processes.

Over all, during the CO_2-ESGR processes, the permeability of the reservoir is influenced by multiple factors, thus, the fluid flow behavior of shale is controlled by the complex coupled thermo-hydro-mechanical-chemical (THMC) processes associated with CO_2 injection. The coupling framework and relationship are shown in Fig. 12. In future, the coupled multicomponent, multiphase flow behaviors considering the phase change of CO_2 in shale during the CO_2-ESGR process should be further investigated.

2.6 CO_2 sequestration in shale formations

Shale gas reservoirs have proven the ability to retain the gas over geologic timescales. The generally low permeability of shales is ideal for caprocks, which contain injected CO_2. As long as the caprocks are not damaged by the hydraulic fractures introduced for shale gas production, CO_2 could be securely retained as shale gas has been. Recent studies have reported that the shale gas reservoir has a potential for large-scale sequestration of CO_2 with multiple sequestration mechanisms (Zhou et al., 2012; Edwards et al., 2015; Levine et al., 2016). Edwards et al. (2015) estimated that the CO_2 storage capacity is 7.2-9.6 Gt in the Marcellus shale and 2.1-3.1 Gt in the Barnett shale. Tao and Clarens (2013) estimated that 10.4-18.4 Gt of CO_2 could be stored in the Marcellus shale by 2030, and Nuttall et al. (2005) estimated that 28 Gt could be stored in the Devonian shale.

In shale gas plays, CH_4 exists both as a free phase in pores and fractures and as adsorbed gas on organic matter or clay surfaces. After the CH_4 is extracted, CO_2 could be stored by the same mechanisms as CH_4 in two populations. Theoretically, the total amount of CO_2, which can be stored, may be estimated from the CH_4 produced, as follows:

$$Q_{CO_2} = \left[\left(\frac{\rho_{CO_2}}{\rho_{CH_4}} \right) X + \left(\frac{A_{CO_2}}{A_{CH_4}} \right) (1-X) \right] Q_{CH_4} \quad (1)$$

where Q_{CO_2} is the molar ratio of CO_2 to be stored over CH_4 produced. X is the fraction of free-phase CH_4 in the shale formation, ρ_{CO_2} and ρ_{CH_4} are the molar density of CO_2 and CH_4, respectively. A_{CO_2} and A_{CH_4} are the adsorption affinity of CO_2 and CH_4 on the shale, respectively. As CO_2 has higher molar density and adsorption affinity than CH_4, the produced methane could be displaced by a greater amount of CO_2 in the depleted shale gas reservoirs. First, we consider the space for free phase CO_2, the density of gases is dependent on pressure
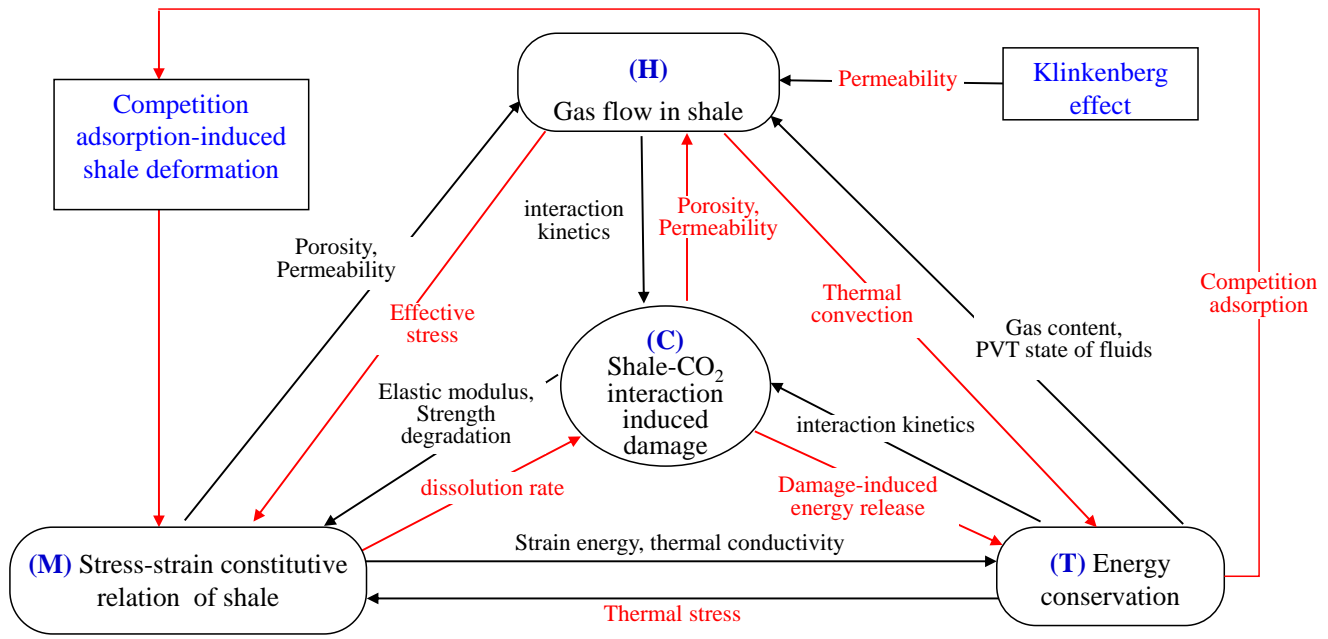
Fig. 12. Coupled THMC processes during the CO$_2$-ESGR.

and temperature, which are functions of burial depth of shale gas reservoirs. In the depth range 1,000 to 5,000 m of the largest shale gas reservoirs in Chongqing, China, the molar density ratio ρ_{CO_2}/ρ_{CH_4} (calculated assuming 0.01 MPa/m pressure gradient, 0.024 °C/m temperature gradient and 20 °C ground temperature) varies from 1.35 to 2.8, which means that one mole of produced CH$_4$ could create the space for 1.35-2.8 moles of CO$_2$. As for the adsorption affinity ratio of CO$_2$ over CH$_4$ on shale, the value varies between 2.1 and 7.2 for several shale samples from China (Zhou et al., 2018a), which means that the 2.1-7.2 moles of CO$_2$ can be adsorbed for one mole of CH$_4$ produced. As the adsorption affinity ratio of CO$_2$ over CH$_4$ is also a function of reservoir pressure and temperature, pore structure and mineral composition of shale, and shale is an extremely heterogeneous and anisotropic material, the CO$_2$ storage capacity of shale gas reservoirs should be evaluated targeting the specific reservoir characteristics for specific CO$_2$-ESGR and CO$_2$ sequestration projects.

In addition, it should be noted that in the Eq. (1), there are only two trapping mechanisms were considered: The structural mechanism (free phase CO$_2$) and adsorption mechanism. However, in the reservoir conditions, mineral trapping may also occur. Interactions between ScCO$_2$ and minerals of shale are important for the when CO$_2$ is injected into shale formations for storage and as working fluids for fracturing and enhanced shale gas recovery. In conventional wisdom, it is usually considered that only typical swelling clays such as smectites can take up CO$_2$ into interlayers at the reservoir condition. However, Wan et al. (2018) found that CO$_2$ can enter muscovite interlayers without bulk interlayer expansion, and the amount of CO$_2$ uptake by muscovite (a conservative proxy for illite and a non-swelling phyllosilicate) far exceeds the maximum adsorption capacity of its external surface area, which constitutes a previously unrecognized potential trapping

mechanism. As the non-swelling illitic clay is the major clay mineral in shale, the unexpected uptake of CO$_2$ by non-swelling phyllosilicates may significantly contribute to CO$_2$ storage capacity in shale. Thus, the CO$_2$ sequestration mechanism in shale formation warrants further indepth studies when estimating the CO$_2$ storage capacity.

2.7 Field test

The first ScCO$_2$ fracturing experiment with continental shale gas was successfully conducted in the Yan-2011 shale gas well in Shaanxi Province, China (Li and Kang, 2018). The field test confirmed that ScCO$_2$ fracturing technology can effectively form a complex fracture network and increase stimulated reservoir volume, as compared to the results of conventional hydraulic fracturing. After ScCO$_2$ fracturing, a continuous test of flowback indicated that the CO$_2$-retention rate was 39.5% and the shale gas production rate was increased 1.5 times. The test results show that ScCO$_2$ fracturing for shale reservoirs is an efficient method for enhancing gas recovery, reducing water consumption, and achieving geological sequestration of CO$_2$. So far, ScCO$_2$ fracturing has been applied in several other shale gas wells, enhanced shale gas recovery and CO$_2$ sequestration were also achieved in these wells, which confirmed the commercial application prospect of the technology as its superiority in improving shale gas recovery, CO$_2$ utilization and geological storage, and water conservation.

3. Conclusions

In this paper, the advancements in the integration technology of ScCO$_2$ fracturing, enhanced shale gas recovery and CO$_2$ sequestration were reviewed. The progress of some key

scientific problems associated with the technique such as the mechanism of $ScCO_2$ drilling and completion technologies, the supercritical carbon dioxide fracturing technology, the competition adsorption behaviors of CO_2/CH_4 in shale, the coupled multiphase and multicomponent CO_2/CH_4 flow during the CO_2 enhanced shale gas recovery process and the CO_2 sequestration potential in shale formation were discussed. The accomplishments via laboratory experiments, theoretical model development and field validation studies confirmed that the $ScCO_2$ fracturing enhanced shale gas recovery and CO_2 sequestration operations has commercial application prospect. However, as with any emerging technology, and particularly in a complex reservoir environment, many technical unknowns and challenges remain. Future work should be conducted to address these unknowns and challenges, and ultimately lead to commercial application of the technology.

Acknowledgments

References

Ambrose, R.J., Hartman, R.C., Akkutlu, I.Y. Multi-component sorbed phase considerations for shale gas-in-place calculations. Paper SPE 141416 Presented at SPE Production and Operations Symposium, Oklahoma City, Oklahoma, USA, 27-29 March, 2011.

Ao, X., Lu, Y., Tang, J., et al. Investigation on the physics structure and chemical properties of the shale treated by supercritical CO_2. J. CO_2 Util. 2017, 20: 274-281.

Bhandari, A.R., Flemings, P.B., Polito, P.G., et al. Anisotropy and stress dependence of permeability in the Barnett shale. Transp. Porous Media 2015, 108(2): 393-411.

Bi, H., Jiang, Z., Li, J., et al. Ono-Kondo model for supercritical shale gas storage: A case study of Silurian Longmaxi shale in southeast Chongqing, China. Energy Fuels 2017, 31(3): 2755-2764.

Cai, C., Kang, Y., Wang, X., et al. Mechanism of supercritical carbon dioxide (SC-CO_2) hydro-jet fracturing. J. CO_2 Util. 2018, 26: 575-587.

Cai, C., Kang, Y., Wang, X., et al. Experimental study on shale fracturing enhancement by using multi-times pulse supercritical carbon dioxide (SC-CO_2) jet. J. Pet. Sci. Eng. 2019, 178: 948-963.

Cai, C., Wang, X., Mao, S., et al. Heat transfer characteristics and prediction model of supercritical carbon dioxide (SC-CO_2) in a vertical tube. Energies 2017, 10(11): 1870.

Cancino, O.P.O., Pérez, D.P., Pozo, M., et al. Adsorption of pure CO_2 and a CO_2/CH_4 mixture on a black shale sample: Manometry and microcalorimetry measurements.
J. Pet. Sci. Eng. 2017, 159: 307-313.

Charoensuppanimit, P., Mohammad, S.A., Gasem, K.A.M. Measurements and modeling of gas adsorption on shales. Energy Fuels 2016, 30(3): 2309-2319.

Chen, M., Kang, Y., Zhang, T., et al. Methane adsorption behavior on shale matrix at in-situ pressure and temperature conditions: Measurement and modeling. Fuel 2018b, 228: 39-49.

Chen, T., Feng, X., Cui, G., et al. Experimental study of permeability change of organic-rich gas shales under high effective stress. J. Nat. Gas Sci. Eng. 2019, 64: 1-14.

Chen, T., Feng, X., Pan, Z. Experimental study of swelling of organic rich shale in methane. Int. J. Coal Geol. 2015a, 150-151: 64-73.

Chen, T., Feng, X., Pan, Z. Experimental study on kinetic swelling of organic-rich shale in CO_2, CH_4 and N_2. J. Nat. Gas Sci. Eng. 2018a, 55: 406-417.

Chen, Y., Nagaya, Y., Ishida, T. Observations of fractures induced by hydraulic fracturing in anisotropic granite. Rock Mech. Rock Eng. 2015b, 48(4): 1455-1461.

Cui, X., Bustin, A.M.M., Bustin, R.M. Measurements of gas permeability and diffusivity of tight reservoir rocks: Different approaches and their applications. Geofluids 2009, 9(3): 208-223.

Dai, C., Wang, T., Zhao, M., et al. Impairment mechanism of thickened supercritical carbon dioxide fracturing fluid in tight sandstone gas reservoirs. Fuel 2018, 211: 60-66.

Dehghanpour, H., Zubair, H.A., Chhabra, A., et al. Liquid intake of organic shales. Energy Fuels 2012, 26(9): 5750-5758.

Distefano, V.H., Mcfarlane, J., Stack, A.G., et al. Solvent-pore interactions in the Eagle Ford shale formation. Fuel 2019, 238: 298-311.

Duan, S., Gu, M., Du, X., et al. Adsorption equilibrium of CO_2 and CH_4 and their mixture on Sichuan Basin shale. Energy Fuels 2016, 30(3): 2248-2256.

Du, M., Sun, X., Dai, C., et al. Laboratory experiment on a toluene-polydimethyl silicone thickened supercritical carbon dioxide fracturing fluid. J. Pet. Sci. Eng. 2018, 166: 369-374.

Du, Y., Wang, R., Ni, H., et al. Determination of rock-breaking performance of high-pressure supercritical carbon dioxide jet. J. Hydrodyn. Ser. B 2012, 24(4): 554-560.

Edwards, R.W.J., Celia, M.A., Bandilla, K.W., et al. A model to estimate carbon dioxide injectivity and storage capacity for geological sequestration in shale gas wells. Environ. Sci. Technol. 2015, 49(15): 9222-9229.

EIA. World shale gas resources: An initial assessment of 14 regions outside the United States. Energy Information Administration, Washington, USA, 2011.

Estrada, J.M., Bhamidimarri, R. A review of the issues and treatment options for wastewater from shale gas extraction by hydraulic fracturing. Fuel 2016, 182: 292-303.

Fathi, E., Akkutlu, I.Y. Multi-component gas transport and adsorption effects during CO_2 injection and enhanced shale gas recovery. Int. J. Coal Geol. 2014, 123: 52-61.

Feng, G., Kang, Y., Sun, Z., et al. Effects of supercritical CO_2 adsorption on the mechanical characteristics and failure mechanisms of shale. Energy 2019, 173: 870-882.

Goodman, A., Sanguinito, S., Tkach, M., et al. Investigating the role of water on CO_2-Utica Shale interactions for carbon storage and shale gas extraction activities-Evidence for pore scale alterations. Fuel 2019, 242: 744-755.

Gregory, K.B., Vidic, R.D., Dzombak, D.A. Water management challenges associated with the production of shale gas by hydraulic fracturing. Elements 2011, 7(3): 181-186.

Gu, M., Xian, X., Duan, S., et al. Influences of the composition and pore structure of a shale on its selective adsorption of CO_2 over CH_4. J. Nat. Gas Sci. Eng. 2017, 46: 296-306.

Gutierrez, M., Katsuki, D., Tutuncu, A. Determination of the continuous stress dependent permeability, compressibility and poroelasticity of shale. Mar. Pet. Geol. 2015, 68: 614-628.

Ha, S.J., Choo, J., Yun, T.S. Liquid CO_2 fracturing: Effect of fluid permeation on the breakdown pressure and cracking behavior. Rock Mech. Rock Eng. 2018, 51(11): 3407-3420.

He, Z., Li, G., Tian, S., et al. SEM analysis on rock failure mechanism by supercritical CO_2 jet impingement. J. Pet. Sci. Eng. 2016a, 146: 111-120.

He, Z., Li, G., Wang, H., et al. Numerical simulation of the abrasive supercritical carbon dioxide jet: The flow field and the influencing factors. J. Hydrodyn. 2016b, 28(2): 238-246.

He, Z., Tian, S., Li, G., et al. The pressurization effect of jet fracturing using supercritical carbon dioxide. J. Nat. Gas Sci. Eng. 2015, 27: 842-851.

Heller, R., Vermylen, J., Zoback, M. Experimental investigation of matrix permeability of gas shales. AAPG Bull. 2014a, 98(5): 975-995.

Heller, R., Zoback, M. Adsorption of methane and carbon dioxide on gas shale and pure mineral samples. J. Unconv. Oil Gas Res. 2014b, 8: 14-24.

Hong, L., Jain, J., Romanov, V., et al. An investigation of factors affecting the interaction of CO_2 and CH_4 on shale in Appalachian Basin. J. Unconv. Oil Gas Res. 2016, 14: 99-112.

Hou, L., Jiang, T., Liu, H., et al. An evaluation method of supercritical CO_2 thickening result for particle transporting. J. CO_2 Util. 2017a, 21: 247-252.

Hou, L., Sun, B., Geng, X., et al. Study of the slippage of particle/supercritical CO_2 two-phase flow. J. Supercrit. Fluids 2017b, 120: 173-180.

Hou, L., Sun, B., Wang, Z., et al. Experimental study of particle settling in supercritical carbon dioxide. J. Supercrit. Fluids 2015, 100: 121-128.

Hu, H., Hao, F., Guo X., et al. Investigation of methane sorption of overmature Wufeng-Longmaxi shale in the Jiaoshiba area, Eastern Sichuan Basin, China. Mar. Pet. Geol. 2018, 91: 251-261.

Huang, F., Hu, B. Macro/microbehavior of shale rock under the dynamic impingement of a high-pressure supercritical carbon dioxide jet. RSC Adv. 2018a, 8: 38065-38074.

Huang, L., Ning, Z., Wang, Q., et al. Molecular simulation of adsorption behaviors of methane, carbon dioxide and their mixtures on kerogen: Effect of kerogen maturity and moisture content. Fuel 2018c, 211: 159-172.

Huang, M., Kang, Y., Wang, X., et al. Experimental investigation on the rock erosion characteristics of a self-excited oscillation pulsed supercritical CO_2 jet. Appl. Therm. Eng. 2018b, 139: 445-455.

Huang, M., Kang, Y., Wang, X., et al. Analysis of the flow characteristics of the high-pressure supercritical carbon dioxide jet. J. Hydrodyn. 2019, 31(2): 389-399.

Hui, D., Pan, Y., Luo, P., et al. Effect of supercritical CO_2 exposure on the high-pressure CO_2 adsorption performance of shales. Fuel 2019, 247: 57-66.

Hu, Y., Kang, Y., Wang, X., et al. Experimental and theoretical analysis of a supercritical carbon dioxide jet on wellbore temperature and pressure. J. Nat. Gas Sci. Eng. 2016, 36: 108-116.

Inui, S., Ishida, T., Nagaya, Y., et al. AE monitoring of hydraulic fracturing experiments in granite blocks using supercritical CO_2, water and viscous oil. Paper ARMA-2014-7163 Presented at 48th U.S. Rock Mechanics/Geomechanics Symposium, Minneapolis, Minnesota, 1-4 June, 2014.

Ishida, T., Aoyagi, K., Niwa, T., et al. Acoustic emission monitoring of hydraulic fracturing laboratory experiment with supercritical and liquid CO_2. Geophys. Res. Lett. 2012, 39(16): L16309.

Ishida, T., Chen, Y., Bennour, Z., et al. Features of CO_2 fracturing deduced from acoustic emission and microscopy in laboratory experiments. J. Geophys. Res. 2016, 121(11): 8080-8098.

Jia, B., Tsau, J.S., Barati, R. A workflow to estimate shale gas permeability variations during the production process. Fuel 2018b, 220: 879-889.

Jia, B., Tsau, J.S., Barati, R. Different flow behaviors of low-pressure and high-pressure carbon dioxide in shales. SPE J. 2018c, 23(4): 1452-1468.

Jia, B., Tsau, J.S., Barati, R. A review of the current progress of CO_2 injection EOR and carbon storage in shale oil reservoirs. Fuel 2019, 236: 404-427.

Jia, Y., Lu, Y., Elsworth, D., et al. Surface characteristics and permeability enhancement of shale fractures due to water and supercritical carbon dioxide fracturing. J. Pet. Sci. Eng. 2018a, 165: 284-297.

Jiang, Y., Luo, Y., Lu, Y., et al. Effects of supercritical CO_2 treatment time, pressure, and temperature on microstructure of shale. Energy 2016, 97: 173-181.

Jiang, Y., Qin, Q., Kang, Z., et al. Experimental study of supercritical CO_2 fracturing on initiation pressure and fracture propagation in shale under different triaxial stress conditions. J. Nat. Gas Sci. Eng. 2018, 55: 382-394.

Jing, Z., Feng, C., Wang, X., et al. Effects of temperature and pressure on rheology and heat transfer among bubbles in waterless CO_2-based foam fracturing fluid. J. Nat. Gas Sci. Eng. 2019, 63: 18-26.

Kang, S.M., Fathi, E., Ambrose, R.J., et al. Carbon dioxide storage capacity of organic-rich shales. SPE J. 2011, 16(4): 842-855.

King, G.E. Thirty years of gas shale fracturing: What have we learned? Paper SPE 133456 Presented at SPE Annual Technical Conference and Exhibition, Florence, Italy, 19-22 September, 2010.

Kolle, J.J. Coiled-tubing drilling with supercritical carbon dioxide. Paper SPE 65534 Presented at SPE/CIM International Conference on Horizontal Well Technology, Calgary, Alberta, Canada, 6-8 November, 2000.

Kondash, A.J., Lauer, N.E., Vengosh, A. The intensification of the water footprint of hydraulic fracturing. Sci. Adv. 2018, 4(8): eaar5982.

Kulga, B., Ertekin, T. Numerical representation of multi-component gas flow in stimulated shale reservoirs. J. Nat. Gas Sci. Eng. 2018, 56: 579-592.

Lan, Y., Yang, Z., Wang, X., et al. A review of microscopic seepage mechanism for shale gas extracted by supercritical CO_2 flooding. Fuel 2019, 238: 412-424.

Levine, J.S., Fukai, I., Soeder, D.J., et al. US DOE NETL methodology for estimating the prospective CO_2 storage resource of shales at the national and regional scale. Int. J. Greenhouse Gas Control 2016, 51: 81-94.

Li, J., Yu, T., Liang, X., et al. Insights on the gas permeability change in porous shale. Adv. Geo-Energy Res. 2017, 1(2): 69-73.

Li, M., Ni, H., Xiao, C., et al. Influences of supercritical carbon dioxide jets on damage mechanisms of rock. Arab. J. Sci. Eng. 2018a, 43(5): 2641-2658.

Li, Q., Wang, Y., Wang, F., et al. Effect of a modified silicone as a thickener on rheology of liquid CO_2 and its fracturing capacity. Polymers 2019, 11(3): 540-555.

Li, X., Feng, Z., Han, G., et al. Breakdown pressure and fracture surface morphology of hydraulic fracturing in shale with H_2O, CO_2 and N_2. Geomech. Geophys. Geo-Energy Geo-Res. 2016, 2(2): 63-76.

Li, X., Kang, Y. Enhanced shale gas recovery using supercritical carbon dioxide. Science, 2018, Celebrating 125 Years of Academic Excellence: Wuhan University (1893-2018), 30.

Li, X., Yi, L., Yang, Z., et al. Coupling model for calculation of transient temperature and pressure during coiled tubing drilling with supercritical carbon dioxide. Int. J. Heat Mass Transf. 2018b, 125: 400-412.

Lu, Y., Ao, X., Tang, J., et al. Swelling of shale in supercritical carbon dioxide. J. Nat. Gas Sci. Eng. 2016, 30: 268-275.

Lu, Y., Chen, X., Tang, J., et al. Relationship between pore structure and mechanical properties of shale on supercritical carbon dioxide saturation. Energy 2019, 172: 270-285.

Luo, X., Ren, X., Wang, S. Supercritical CO_2-water-shale interactions and their effects on element mobilization and shale pore structure during stimulation. Int. J. Coal Geol. 2019, 202: 109-127.

Luo, X., Wang, S., Wang, Z., et al. Adsorption of methane, carbon dioxide and their binary mixtures on Jurassic shale from the Qaidam Basin in china. Int. J. Coal Geol. 2015, 150-151: 210-223.

Lyu, Q., Long, X., Ranjith, P.G., et al. A laboratory study of geomechanical characteristics of black shales after sub-critical/super-critical CO_2+brine saturation. Geomech. Geophys. Geo-Energy Geo-Res. 2018a, 4(2): 141-156.

Lyu, Q., Long, X., Ranjith, P.G., et al. Experimental investigation on the mechanical properties of a low-clay shale with different adsorption times in sub-/super-critical CO_2. Energy 2018b, 147: 1288-1298.

Lyu, Q., Ranjith, P.G., Long, X., et al. Experimental investigation of mechanical properties of black shales after CO_2-water-rock interaction. Materials 2016, 9(8): 663.

Lyu, Q., Tan, J., Dick, J.M., et al. Stress-strain modeling and brittleness variations of low-clay shales with CO_2/CO_2-water imbibition. Rock Mech. Rock Eng. 2019, 52: 2039-2052.

Ma, X., Xie, J. The progress and prospects of shale gas exploration and development in southern Sichuan Basin, SW China. Pet. Explor. Dev. 2018, 45(1): 172-182.

Melikoglu, M. Shale gas: Analysis of its role in the global energy market. Renewable Sustainable Energy Rev. 2014, 37: 460-468.

Middleton, R., Carey, J., Currier, R., et al. Shale gas and non-aqueous fracturing fluids: Opportunities and challenges for supercritical CO_2. Appl. Energy 2015, 147: 500-509.

Middleton, R., Viswanathan, H., Currier, R., et al. CO_2 as a fracturing fluid: Potential for commercial-scale shale gas production and CO_2 sequestration. Energy Procedia 2014, 63: 7780-7784.

Miedzińska, D., Lutyński, M. CO_2-CH_4 sorption induced swelling of gas shales: An experimental study on the Silurian shales from the Baltic Basin, Poland. Physicochem. Probl. Miner. Process. 2018, 54(2): 415-427.

Mo, D., Jia, B., Yu, J., et al. Study of nanoparticle-stabilized CO_2 foam for oil recovery at different pressure, temperature, and rock samples. Paper SPE 169110 Presented at SPE Improved Oil Recovery Symposium, Tulsa, Oklahoma, USA, 12-16 April, 2014.

Moghadam, A.A., Chalaturnyk, R. Analytical and experimental investigations of gas-flow regimes in shales considering the influence of mean effective stress. SPE J. 2016, 21(2): 557-572.

Moghaddam, N.R., Jamiolahmady, M. Fluid transport in shale gas reservoirs: Simultaneous effects of stress and slippage on matrix permeability. Int. J. Coal Geol. 2016, 163: 87-99.

Myshakin, E.M., Singh, H., Sanguinito, S., et al. Numerical estimations of storage efficiency for the prospective CO_2 storage resource of shales. Int. J. Greenhouse Gas Control 2018, 76: 24-31.

Nagel, N.B., Sanchez-Nagel, M.A., Zhang, F., et al. Coupled numerical evaluations of the geomechanical interactions between a hydraulic fracture stimulation and a natural fracture system in shale formations. Rock Mech. Rock Eng. 2013, 46(3): 581-609.

Nguyen-Le, V., Shin, N. Development of reservoir economic indicator for Barnett shale gas potential evaluation based on the reservoir and hydraulic fracturing parameters. J. Nat. Gas Sci. Eng. 2019, 66: 159-167.

Nicot, J.P., Scanlon, B.R. Water use for shale-gas production in Texas, US. Environ. Sci. Technol. 2012, 46(6): 3580-3586.

Niu, Y., Yue, C., Li, S., et al. Influencing factors and selection of CH_4 and CO_2 adsorption on Silurian shale in Yibin, Sichuan province of China. Energy Fuels 2018, 32(3): 3202-3210.

Nuttall, B.C., Eble, C., Bustin, R.M., et al. Analysis of Devonian black shales in Kentucky for potential carbon dioxide sequestration and enhanced natural gas production, in Greenhouse Gas Control Technologies 7, edited by Rubin, E.S., Keith, D.W., Gilboy, C.F., et al. Elsevier Science Ltd, Oxford, pp. 2225-2228, 2005.

Osborn, S.G., Vengosh, A., Warner, N.R., et al. Methane contamination of drinking water accompanying gas-well drilling and hydraulic fracturing. Proc. Natl. Acad. Sci. USA 2011, 108(20): 8172-8176.

Pan, Y., Hui, D., Luo, P., et al. Experimental investigation of the geo-chemical interactions between supercritical CO_2 and shale: Implications for CO_2 storage in gas-bearing shale formations. Energy Fuels 2018a, 32(2): 1963-1978.

Pan, Y., Hui, D., Luo, P., et al. Influences of subcritical and supercritical CO_2 treatment on the pore structure characteristics of marine and terrestrial shales. J. CO_2 Util. 2018b, 28: 152-167.

Pan, Z., Ma, Y., Connell, L.D., et al. Measuring anisotropic permeability using a cubic shale sample in a triaxial cell. J. Nat. Gas Sci. Eng. 2015, 26: 336-344.

Pei, P., Ling, K., He, J., et al. Shale gas reservoir treatment by a CO_2-based technology. J. Nat. Gas Sci. Eng. 2015, 26: 1595-1606.

Peng, P., Ju, Y., Wang, Y., et al. Numerical analysis of the effect of natural microcracks on the supercritical CO_2 fracturing crack network of shale rock based on bonded particle models. Int. J. Numer. Anal. Methods Geomech. 2017, 41(18): 1992-2013.

Perera, M.S.A., Ranjith, P.G., Choi, S.K., et al. Investigation of temperature effect on permeability of naturally fractured black coal for carbon dioxide movement: An experimental and numerical study. Fuel 2012, 94: 596-605.

Pluymakers, A., Liu, J., Kohler, F., et al. A high resolution interferometric method to measure local swelling due to CO_2 exposure in coal and shale. Int. J. Coal Geol. 2018, 187: 131-142.

Psarras, P., Holmes, R., Vishal, V., et al. Methane and CO_2 adsorption capacities of kerogen in the Eagle Ford shale from molecular simulation. Accounts Chem. Res. 2017, 50(8): 1818-1828.

Qi, R., Ning, Z., Wang, Q., et al. Sorption of methane, carbon dioxide, and their mixtures on shales from Sichuan Basin, China. Energy Fuels 2018, 32(3): 2926-2940.

Qin, C., Jiang, Y., Luo, Y., et al. Effect of supercritical carbon dioxide treatment time, pressure, and temperature on shale water wettability. Energy Fuels 2017, 31(1): 493-503.

Rafiee, M., Soliman, M.Y., Pirayesh, E., et al. Geomechanical considerations in hydraulic fracturing designs. Paper SPE 162637 Presented at SPE Canadian Unconventional Resources Conference, Calgary, Alberta, Canada., 30 October-1 November, 2012.

Rahimi-Aghdam, S., Chau, V.T., Lee, H., et al. Branching of hydraulic cracks enabling permeability of gas or oil shale with closed natural fractures. Proc. Natl. Acad. Sci. USA 2019, 116(5): 1532-1537.

Ren, W., Tian, S., Li, G., et al. Modeling of mixed-gas adsorption on shale using hPC-SAFT-MPTA. Fuel 2017, 210: 535-544.

Rexer, T.F.T., Benham, M.J., Aplin, A.C., et al. Methane adsorption on shale under simulated geological temperature and pressure conditions. Energy Fuels 2013, 27(6): 3099-3109.

Rezaee, R., Saeedi, A., Iglauer, S., et al. Shale alteration after exposure to supercritical CO_2. Int. J. Greenhouse Gas Control 2017, 62: 91-99.

Ribeiro, L.H., Li, H., Bryant, J.E. Use of a CO_2-hybrid fracturing design to enhance production from unpropped-fracture networks. SPE Prod. Oper. 2017, 32(1): 28-40.

Rutqvist, J., Rinaldi, A.P., Cappa, F., et al. Modeling of fault activation and seismicity by injection directly into a fault zone associated with hydraulic fracturing of shale-gas reservoirs. J. Pet. Sci. Eng. 2015, 127: 377-386.

Sanguinito, S., Goodman, A., Tkach, M., et al. Quantifying dry supercritical CO_2-induced changes of the Utica shale. Fuel 2018, 226: 54-64.

Scanlon, B.R., Reedy, R.C., Nicot, J.P. Comparison of water use for hydraulic fracturing for unconventional oil and gas versus conventional oil. Environ. Sci. Technol. 2014, 48(20): 12386-12393.

Shi, H., Li, G., He, Z., et al. Design of experimental setup for supercritical CO_2 jet under high ambient pressure conditions. Rev. Sci. Instrum. 2016, 87(12): 125115.

Singh, H., Cai, J. A mechanistic model for multi-scale sorption dynamics in shale. Fuel 2018, 234: 996-1014.

Song, W., Ni, H., Wang, R., et al. Pressure controlling method for managed pressure drilling with supercritical carbon dioxide as the circulation fluid. Pet. Explor. Dev. 2016, 43(5): 857-862.

Song, X., Li, G., Guo, B., et al. Transport feasibility of proppant by supercritical carbon dioxide fracturing in reservoir fractures. J. Hydrodyn. 2018a, 30(3): 507-513.

Song, X., Lv, X., Shen, Y., et al. A modified supercritical Dubinin-Radushkevich model for the accurate estimation of high pressure methane adsorption on shales. Int. J. Coal Geol. 2018b, 193: 1-15.

Sun, B., Wang, J., Wang, Z., et al. Calculation of proppant-carrying flow in supercritical carbon dioxide fracturing fluid. J. Pet. Sci. Eng. 2018b, 166: 420-432.

Sun, H., Yao, J., Gao, S., et al. Numerical study of CO_2 enhanced natural gas recovery and sequestration in shale gas reservoirs. Int. J. Greenhouse Gas Control 2013, 19: 406-419.

Sun, X., Ni, H., Wang, R., et al. Characteristic study on supercritical carbon dioxide impinging jet: Calculation and stagnation properties analysis. J. Pet. Sci. Eng. 2018a, 162: 532-538.

Tang, X., Ripepi, N., Luxbacher, K., et al. Adsorption models for methane in shales: Review, comparison and application. Energy Fuels 2017a, 31(10): 10787-10801.

Tang, X., Ripepi, N., Stadie, N.P., et al. A dual-site Langmuir equation for accurate estimation of high pressure deep shale gas resources. Fuel 2016, 185: 10-17.

Tang, X., Ripepi, N., Stadie, N.P., et al. Thermodynamic analysis of high pressure methane adsorption in Longmaxi shale. Fuel 2017b, 193: 411-418.

Tao, Z., Clarens, A. Estimating the carbon sequestration capacity of shale formations using methane production rates. Environ. Sci. Technol. 2013, 47(19): 11318-11325.

Vengosh, A., Jackson, R.B., Warner, N., et al. A critical review of the risks to water resources from unconventional shale gas development and hydraulic fracturing in the United States. Environ. Sci. Technol. 2014, 48(15): 8334-8348.

Wan, J., Tokunaga, T.K., Ashby, P.D., et al. Supercritical CO_2 uptake by nonswelling phyllosilicates. Proc. Natl. Acad. Sci. USA 2018, 115(5): 873-878.

Wang, F., Pan, Z., Zhang, S. Coupled thermo-hydro-chemical modeling of fracturing-fluid leakoff in hydraulically fractured shale gas reservoirs. J. Pet. Sci. Eng. 2018b, 161: 17-28.

Wang, H., Li, G., He, Z., et al. Experimental investigation on abrasive supercritical CO_2 jet perforation. J. CO_2 Util. 2018a, 28: 59-65.

Wang, H., Li, G., Shen, Z. A feasibility analysis on shale gas exploitation with supercritical carbon dioxide. Energy Source. Part A 2012, 34(15): 1426-1435.

Wang, H., Li, G., Shen, Z., et al. Experiment on rock breaking with supercritical carbon dioxide jet. J. Pet. Sci. Eng. 2015a, 127: 305-310.

Wang, H., Li, G., Shen, Z., et al. Expulsive force in the development of CO_2 sequestration: Application of SC-CO_2 jet in oil and gas extraction. Front. Energy 2019b, 13(1): 1-8.

Wang, L., Yao, B., Xie, H., et al. CO_2 injection-induced fracturing in naturally fractured shale rocks. Energy 2017, 139: 1094-1110.

Wang, T., Tian, S., Li, G. Selective adsorption of supercritical carbon dioxide and methane binary mixture in shale kerogen nanopores. J. Nat. Gas Sci. Eng. 2018c, 50: 181-188.

Wang, T., Tian, S., Li, G., et al. Molecular simulation of CO_2/CH_4 competitive adsorption on shale kerogen for CO_2 sequestration and enhanced gas recovery. J. Phys. Chem. C 2018d, 122(30): 17009-17018.

Wang, Y., Ju, Y., Chen, J., et al. Adaptive finite element-discrete element analysis for the multistage supercritical CO_2 fracturing and microseismic modelling of horizontal wells in tight reservoirs consi dering pre-existing fractures and thermal-hydro-mechanical coupling. J. Nat. Gas Sci. Eng. 2019a, 61: 251-269.

Wang, Y., Tsotsis, T.T., Jessen, K. Competitive sorption of methane/ethane mixtures on shale: measurements and modeling. Ind. Eng. Chem. Res. 2015b, 54(48): 12187-12195.

Wang, Y., Zhu, Y., Liu, S., et al. Methane adsorption measurements and modeling for organic-rich marine shale samples. Fuel 2016, 172: 301-309.

Wang, Z., Sun, B., Wang, J., et al. Experimental study on the friction coefficient of supercritical carbon dioxide in pipes. Int. J. Greenhouse Gas Control 2014, 25: 151-161.

Weniger, P., Kalkreuth, W., Busch, A., et al. High-pressure methane and carbon dioxide sorption on coal and shale samples from the Paraná Basin, Brazil. Int. J. Coal Geol. 2010, 84(3-4): 190-205.

Wu, W., Zoback, M.D., Kohli, A.H. The impacts of effective stress and CO_2 sorption on the matrix permeability of shale reservoir rocks. Fuel 2017, 203: 179-186.

Xiong, F., Wang, X., Amooie, M.A., et al. The shale gas sorption capacity of transitional shales in the Ordos Basin, NW China. Fuel 2017, 208: 236-246.

Xiong, J., Liu, X., Liang, L. Experimental study on the pore structure characteristics of the Upper Ordovician Wufeng Formation shale in the southwest portion of the Sichuan Basin, China. J. Nat. Gas Sci. Eng. 2015, 22: 530-539.

Xu, R., Zeng, K., Zhang, C., et al. Assessing the feasibility and CO_2 storage capacity of CO_2 enhanced shale gas recovery using Triple-Porosity reservoir model. Appl. Therm. Eng. 2017, 115: 1306-1314.

Yang, D., Wang, W., Chen, W., et al. Experimental investigation on the coupled effect of effective stress and gas slippage on the permeability of shale. Sci. Rep. 2017, 7: 44696.

Yin, H., Zhou, J., Jiang, Y., et al. Physical and structural changes in shale associated with supercritical CO_2 exposure. Fuel 2016, 184: 289-303.

Yin, H., Zhou, J., Xian, X., et al. Experimental study of the effects of sub- and super-critical CO_2 saturation on the mechanical characteristics of organic-rich shales. Energy 2017, 132: 84-95.

Zhang, S., Xian, X., Zhou, J., et al. Mechanical behaviour of Longmaxi black shale saturated with different fluids: An experimental study. RSC Adv. 2017b, 7: 42946-42955.

Zhang, X., Lu, Y., Tang, J., et al. Experimental study on fracture initiation and propagation in shale using supercritical carbon dioxide fracturing. Fuel 2017a, 190: 370-378.

Zhang, Y., He, J., Li, X., et al. Experimental study on the supercritical CO_2 fracturing of shale considering anisotropic effects. J. Pet. Sci. Eng. 2019, 173: 932-940.

Zhao, Z., Li, X., He, J., et al. A laboratory investigation of fracture propagation induced by supercritical carbon dioxide fracturing in continental shale with interbeds. J. Pet. Sci. Eng. 2018, 166: 739-746.

Zhou, D., Zhang, G., Prasad, M., et al. The effects of temperature on supercritical CO_2 induced fracture: An experimental study. Fuel 2019b, 247: 126-134.

Zhou, D., Zhang, G., Wang, Y., et al. Experimental investigation on fracture propagation modes in supercritical carbon

dioxide fracturing using acoustic emission monitoring. Int. J. Rock Mech. Min. 2018b, 110: 111-119.

Zhou, J., Liu, G., Jiang, Y., et al. Supercritical carbon dioxide fracturing in shale and the coupled effects on the permeability of fractured shale: An experimental study. J. Nat. Gas Sci. Eng. 2016, 36: 369-377.

Zhou, J., Liu, M., Xian, X., et al. Measurements and modelling of CH_4 and CO_2 adsorption behaviors on shales: Implication for CO_2 enhanced shale gas recovery. Fuel 2019a, 251: 293-306.

Zhou, J., Xian, X., Lu, Y., et al. Prediction of carbon dioxide storage capacity in gas shale reservoirs. Symposium on underground disposal of waste, Nanchang, 20-26, 2012.

Zhou, J., Xie, S., Jiang, Y., et al. Influence of supercritical CO_2 Exposure on CH_4 and CO_2 adsorption behaviors of shale: Implications for CO_2 sequestration. Energy Fuels 2018a, 32(5): 6073-6089.

Zhou, J., Yin, H., Tan, J., et al. Pore structural characterization of shales treated by sub-Critical and supercritical CO_2 exposure. J. Nanosci. Nanotechnol. 2017b, 17(9): 6603-6613.

Zhou, Z., Lu, Y., Tang, J., et al. Numerical simulation of supercritical carbon dioxide jet at well bottom. Appl. Therm. Eng. 2017a, 121: 210-217.

Zou, C., Ni, Y., Li, J., et al. The water footprint of hydraulic fracturing in Sichuan Basin, China. Sci. Total Environ. 2018, 630: 349-356.